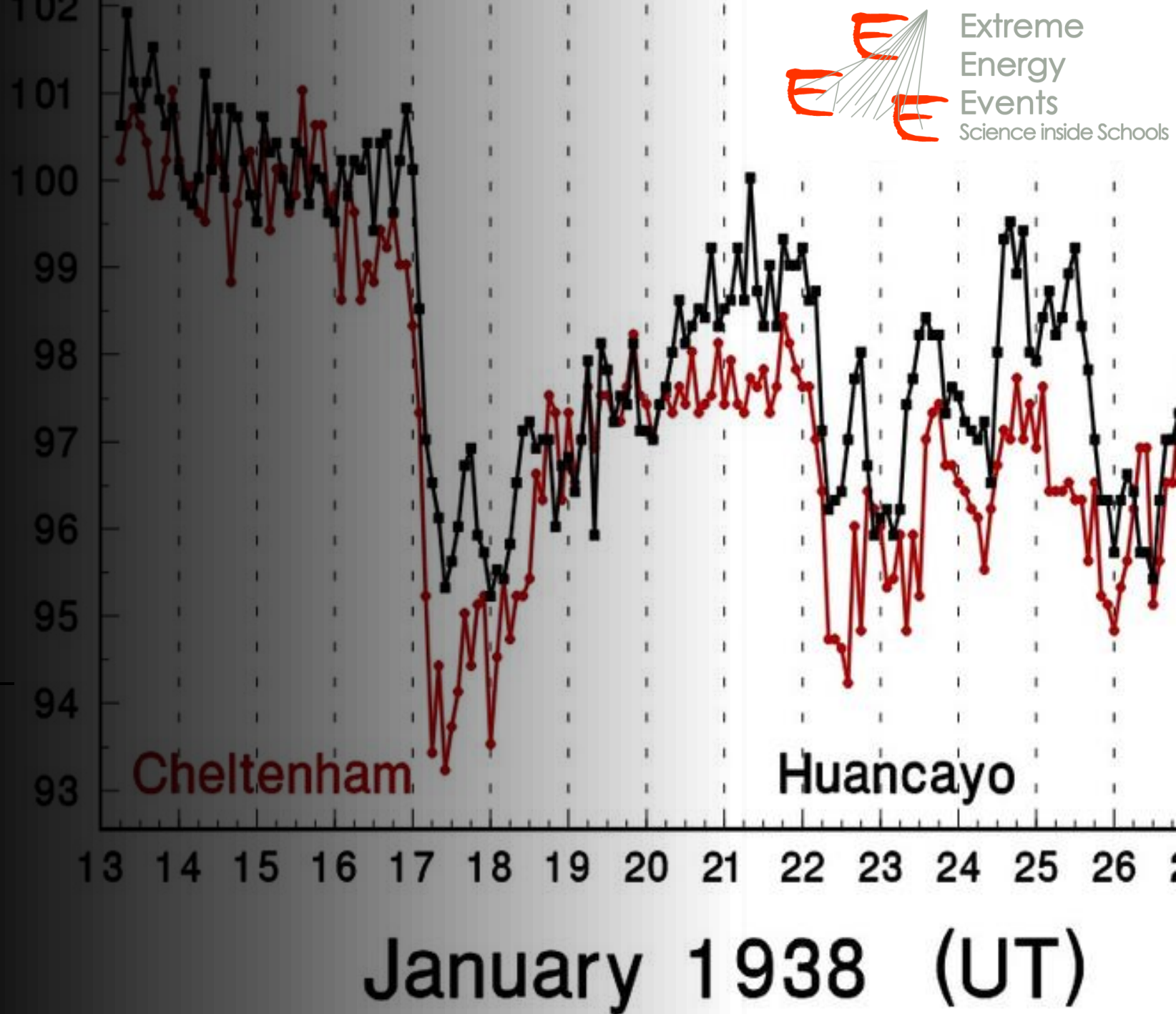
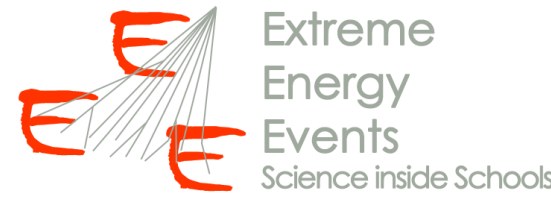




Forbush Decrease

INTERNATIONAL COSMIC DAY 2024

Liceo Scientifico «Banzi Bazoli» - Lecce

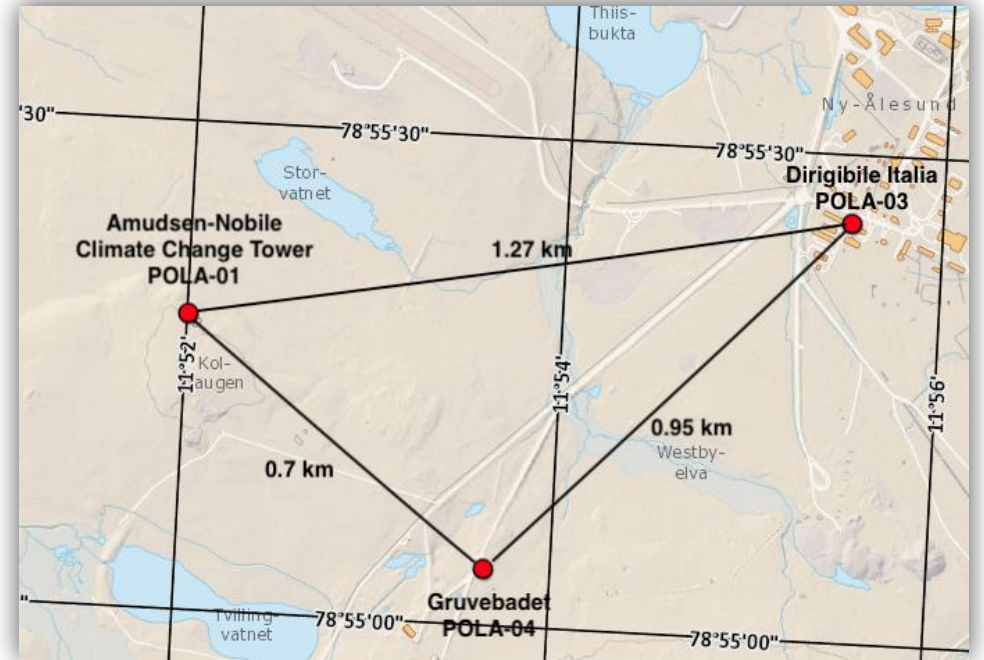


Purpose of the Analysis

With this analysis, we aim to highlight the decrease in cosmic ray flux (**Forbush decrease**), resulting from an increase in solar wind intensity during the geomagnetic storm of May 10–12, 2024.

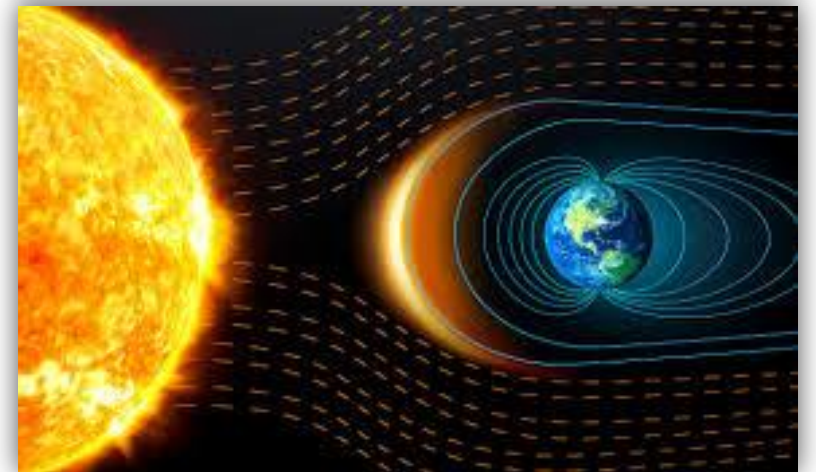
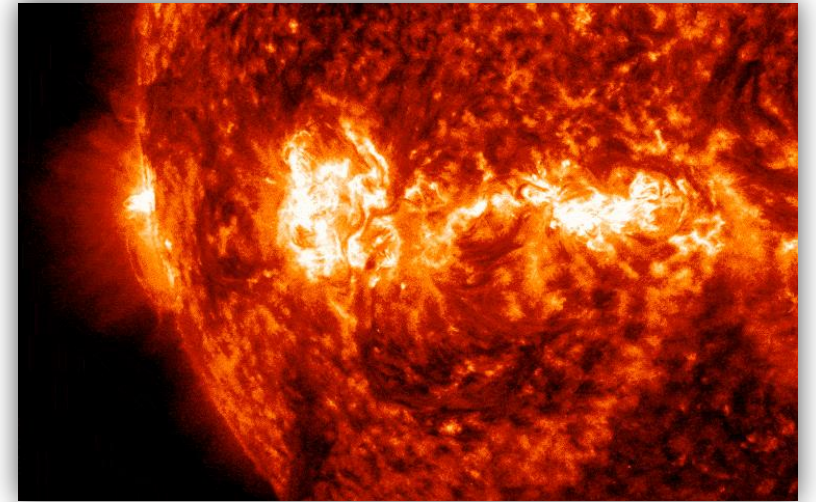
For this purpose, we analyzed data acquired by the scintillator telescopes **POLA-01**, **POLA-03** and **POLA-04**, between April 16th and May 15th

We also used data on geomagnetic activity, provided by the “**World Data Center for Geomagnetism (Kyoto)**”, to relate the flux decrease to geomagnetic field behavior.



Geomagnetic Storm

- A **magnetic storm** is a temporary disturbance in the **geomagnetic field** caused by irregular solar activity, such as **solar flares** followed by **coronal mass ejections** (CME).
- These phenomena lead to an increase in solar wind, which, by interacting with the geomagnetic field, can temporarily modify it, producing effects like the aurora borealis, blackouts and disturbances in telecommunications signals.



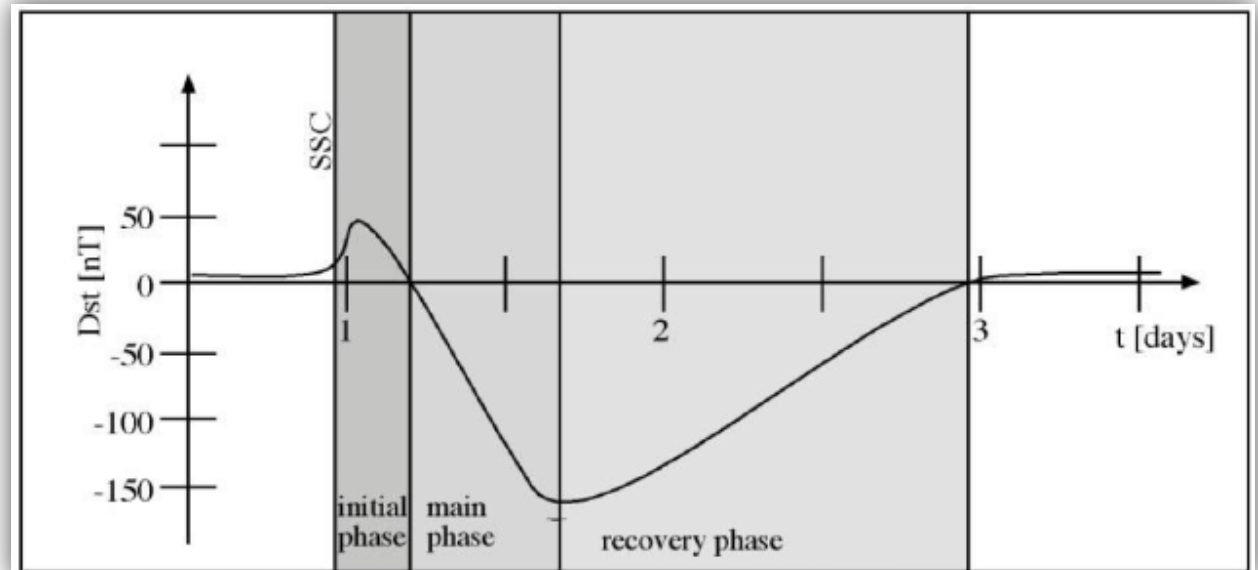
Dst Index

The **Dst index** (Disturbance Storm Time index) is used to assess the intensity of geomagnetic storms. It measures changes in the horizontal component of Earth's magnetic field, particularly in the equatorial region. Dst trend describes the evolution of a magnetic storm:

Initial Phase: A slight positive or stable Dst (~ 0 nT) as solar wind compression enhances Earth's magnetosphere.

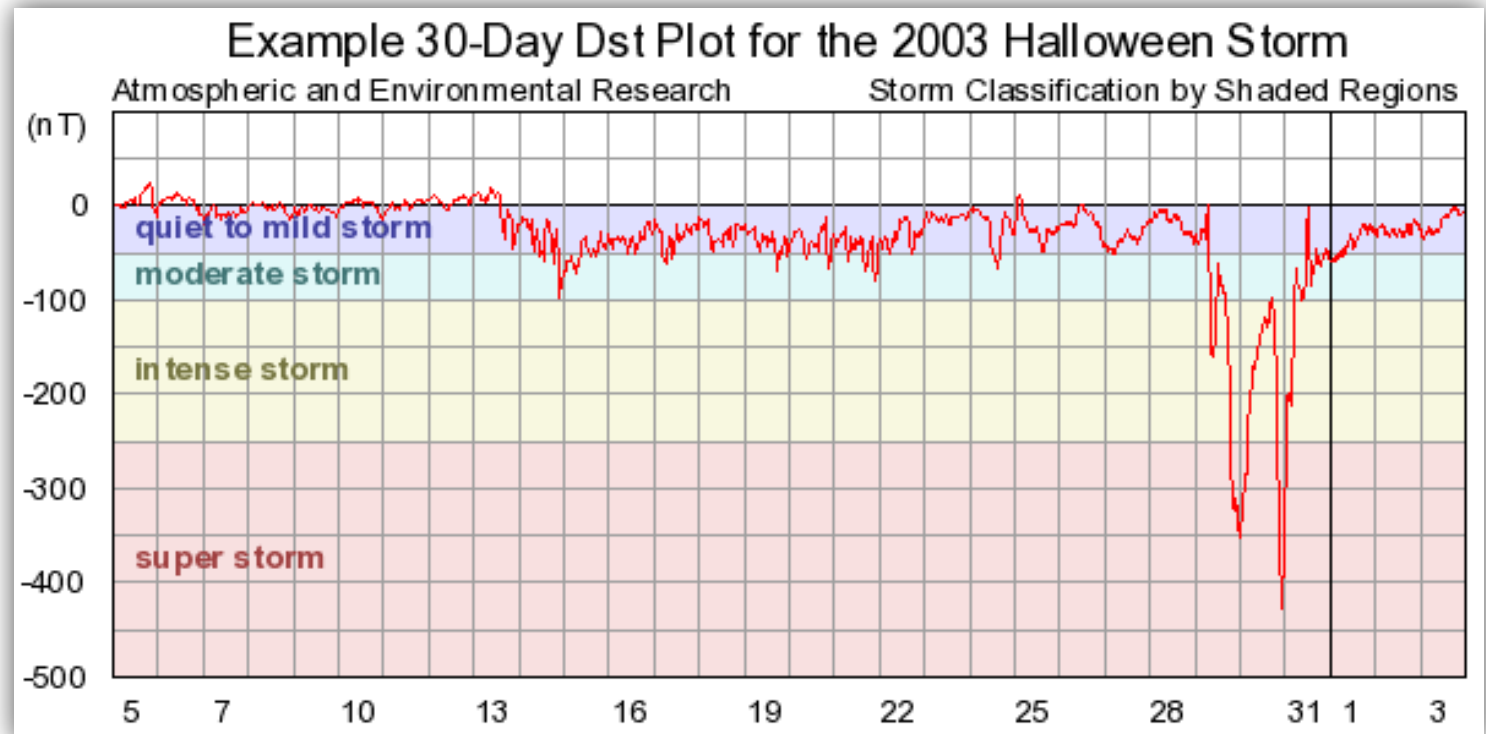
Main Phase: Dst sharply drops (often below -100 nT) due to the increased energy of the ring current from solar wind plasma injection.

Recovery Phase: Dst gradually rises back to baseline as the ring current dissipates over hours to days.

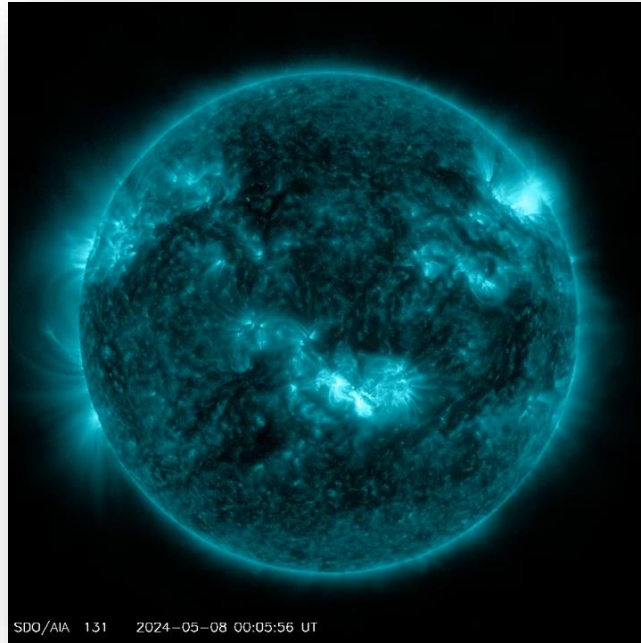


Classifying Geomagnetic Storms with the Dst Index

Negative Dst values indicate the presence and intensity of a geomagnetic storm. The more negative the Dst value, the stronger the storm. Magnetic storms can be classified based on the Dst index, as represented in the figure.

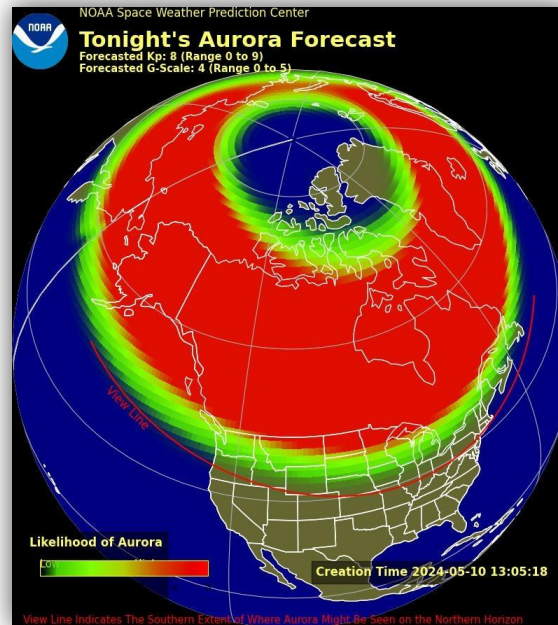


The Magnetic Storm in May 2024

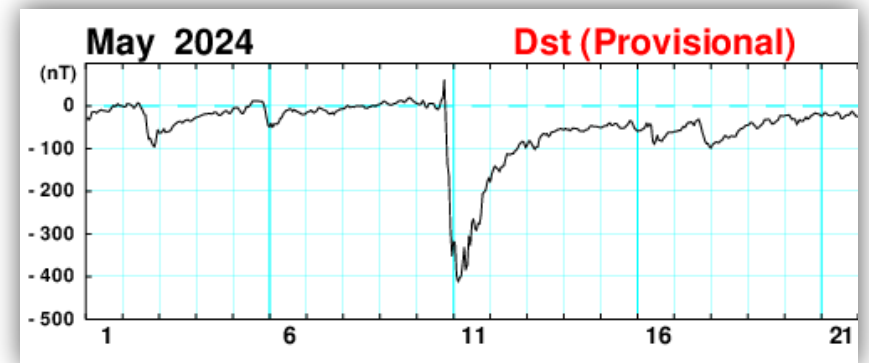


The magnetic storm that occurred from May 10 to May 13, 2024, was caused by extreme solar flares (above, the solar flares of May 8, 2024).

It was the most powerful since the one in March 1989, and it produced auroras at much more equatorial latitudes than usual.



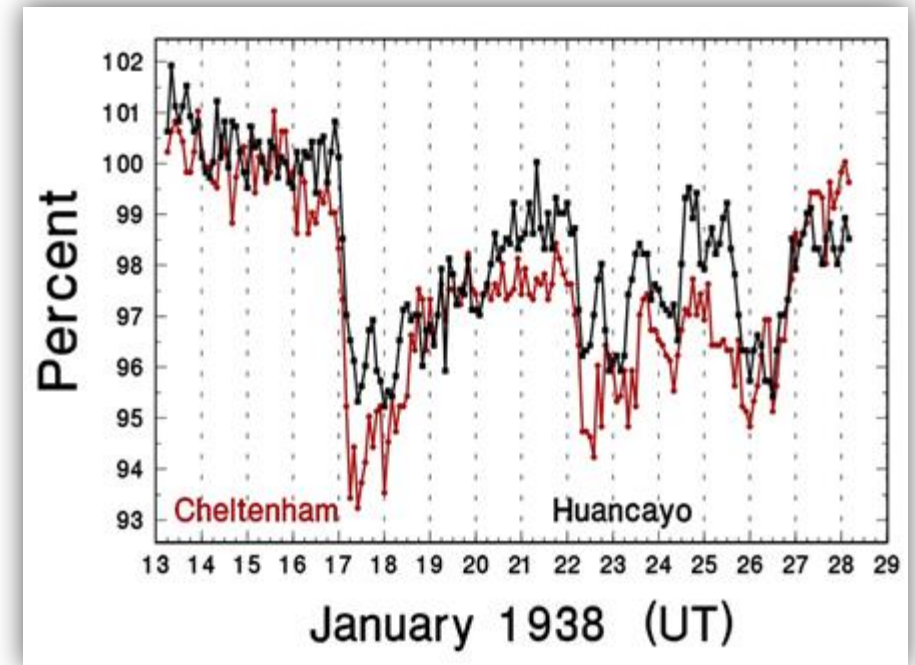
The peak had a Dst index of -412 nT, so it can be classified as an extreme magnetic storm



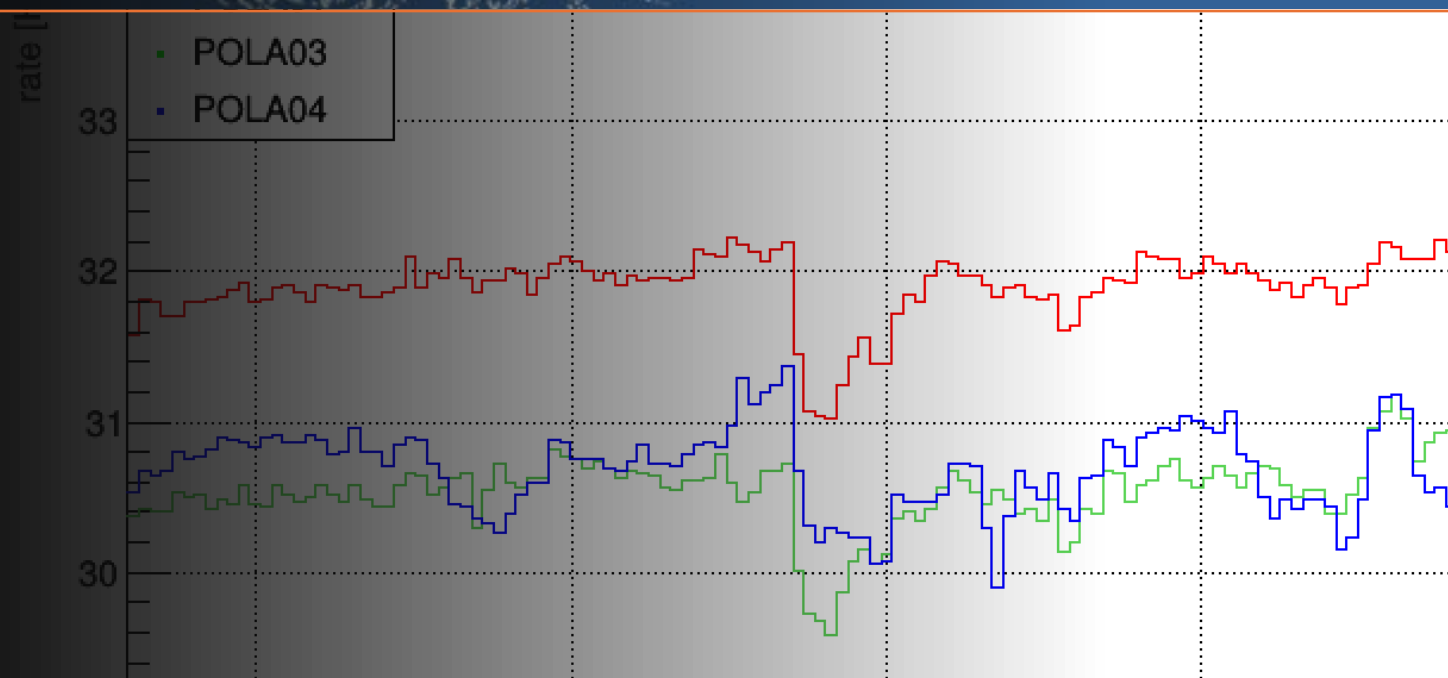
The Forbush Decrease

Cosmic particles are deflected by geomagnetic field, however some penetrate and create particle showers in the upper atmosphere. During a solar storm, the Sun emits plasma that strengthens the magnetic field's shielding effect, preventing some cosmic rays from reaching Earth. This results in a flux decrease called **Forbush Decrease**^{1 2}

- (1) Forbush S. - *On the effects in cosmic-ray intensity observed during the recent magnetic storm*
Phys. Rev., 51 (1937), pp. 1108-1109
- (2) Forbush S. - *On world-wide changes in cosmic-ray intensity*
Phys. Rev., 54 (1938), pp. 975-988



Analysis

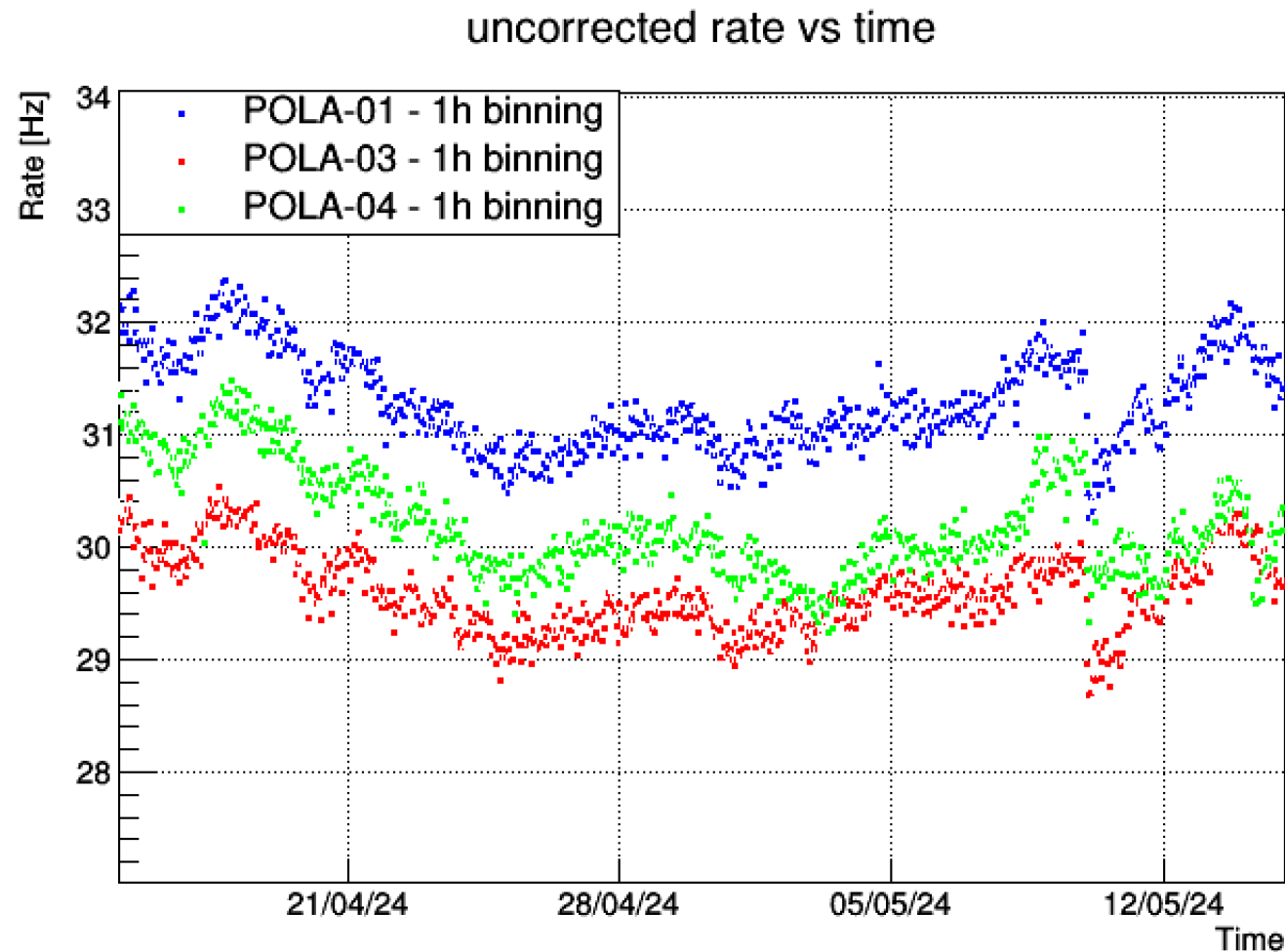


The Dataset

#BinStart,	RateHitEvents,	RateTrackEvents,	Pressure
5.456162050000e+08,	3.216393e+01,	3.216393e+01,	1.012293e+03
5.456162660000e+08,	3.242623e+01,	3.242623e+01,	1.012293e+03
5.456163270000e+08,	3.152459e+01,	3.152459e+01,	1.012293e+03
5.456163880000e+08,	3.242623e+01,	3.242623e+01,	1.012293e+03
5.456164490000e+08,	3.232787e+01,	3.232787e+01,	1.012293e+03
5.456165100000e+08,	3.186885e+01,	3.186885e+01,	1.012293e+03
5.456165710000e+08,	3.404918e+01,	3.404918e+01,	1.012293e+03
5.456166320000e+08,	3.193443e+01,	3.193443e+01,	1.012293e+03
5.456166930000e+08,	3.108197e+01,	3.108197e+01,	1.012293e+03
5.456167540000e+08,	3.336066e+01,	3.336066e+01,	1.012293e+03
5.456168150000e+08,	3.332787e+01,	3.332787e+01,	1.012293e+03
5.456168760000e+08,	3.280328e+01,	3.280328e+01,	1.012293e+03
5.456169370000e+08,	3.132787e+01,	3.132787e+01,	1.012293e+03
5.456169980000e+08,	3.236066e+01,	3.236066e+01,	1.012293e+03
5.456170590000e+08,	3.219672e+01,	3.219672e+01,	1.012293e+03
5.456171200000e+08,	3.139344e+01,	3.139344e+01,	1.012293e+03
5.456171810000e+08,	3.231147e+01,	3.231147e+01,	1.012293e+03
5.456172420000e+08,	3.226229e+01,	3.226229e+01,	1.012293e+03
5.456173030000e+08,	3.322951e+01,	3.322951e+01,	1.012293e+03
5.456173640000e+08,	3.206557e+01,	3.206557e+01,	1.012293e+03
5.456174250000e+08,	3.349180e+01,	3.349180e+01,	1.012293e+03
5.456174860000e+08,	3.311475e+01,	3.311475e+01,	1.012293e+03
5.456175470000e+08,	3.295082e+01,	3.295082e+01,	1.012293e+03

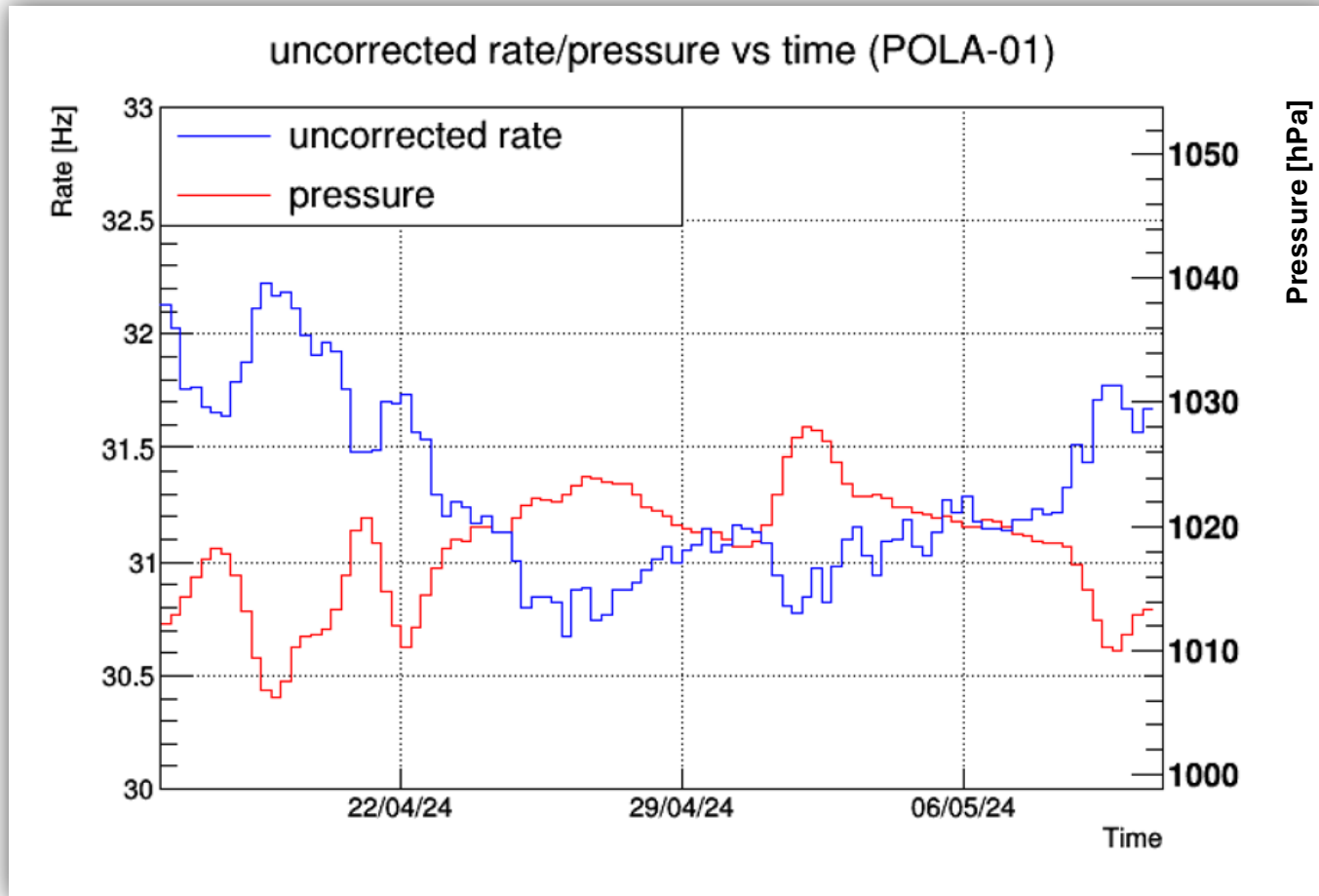
- **BinStart [s]** → Time elapsed since 01/01/2007
- **RateTrackEvents [Hz]** → Reconstructed tracks rate
- **Pressure [hPa]** → atmospheric pressure

Rate of Reconstructed Tracks vs Time



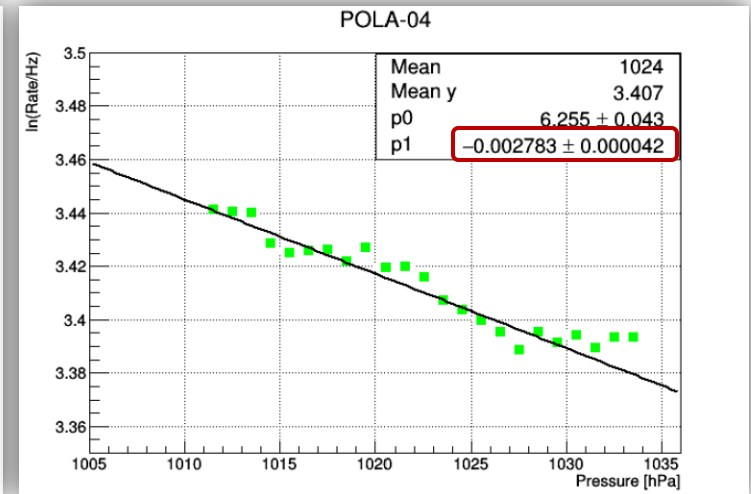
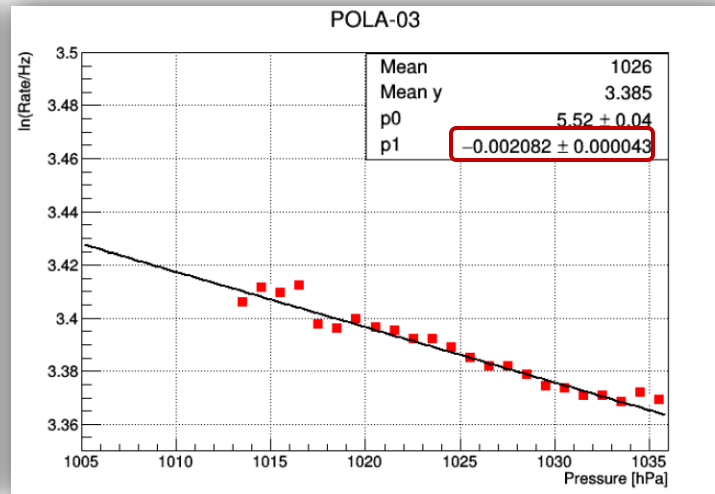
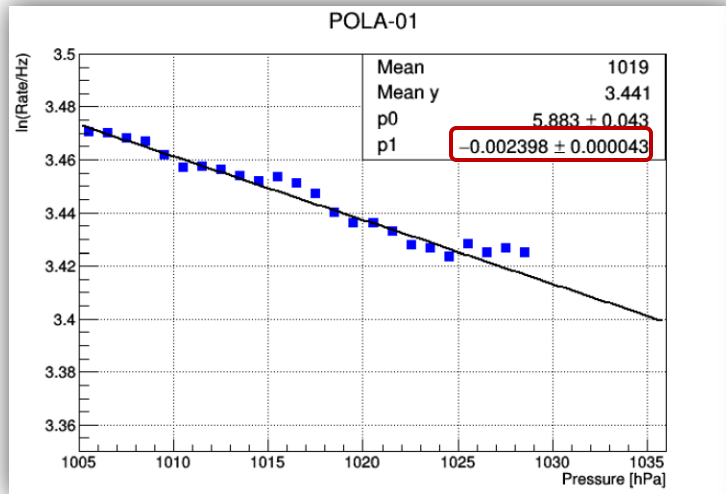
No Forbush decrease is identifiable, because it cannot be distinguished from oscillations caused by pressure variations (barometric effect).

Barometric Effect



If temperature variations are negligible, as the pressure of the atmosphere increases, its density also increases. This results in a greater absorption of secondary cosmic rays by the atmosphere, leading to a decrease in their rate.

Barometric Coefficients



$$r_{cor} = r_{uncor} \cdot \exp[\alpha(P - \bar{P})] \rightarrow \ln(r_{uncor}/\text{Hz}) = \ln(r_{cor}/\text{Hz}) - \alpha(P - \bar{P})$$

$\alpha \rightarrow$ barometric coefficient,

$\bar{P} \rightarrow$ mean pressure

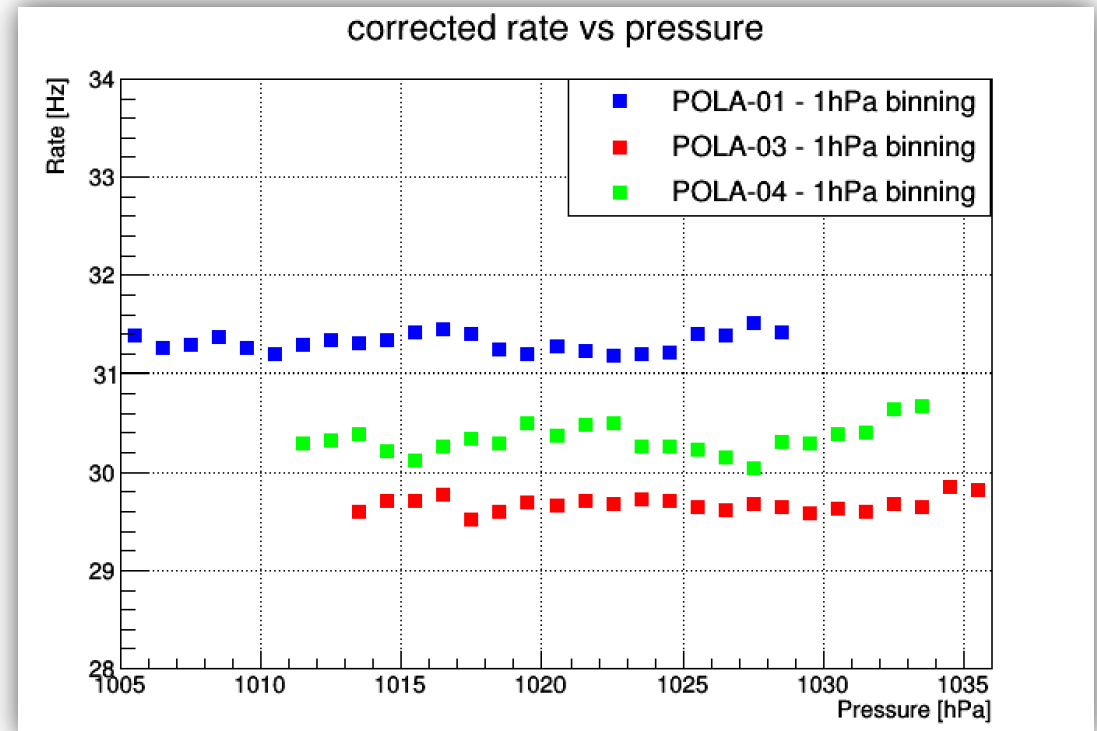
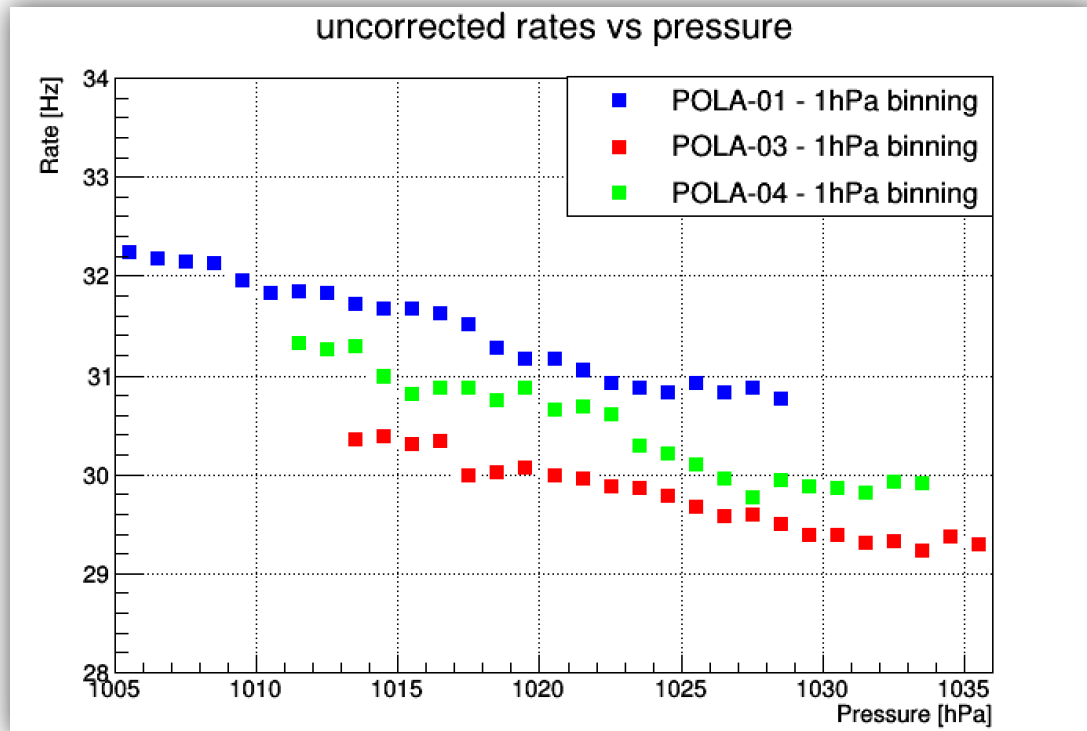
In order to estimate α , we used a data subset not affected by the Forbush decrease, in such a way that the rate is influenced only by pressure.

$$\alpha_{\text{POLA01}} = 0.00240 \text{ hPa}^{-1}$$

$$\alpha_{\text{POLA03}} = 0.00208 \text{ hPa}^{-1}$$

$$\alpha_{\text{POLA04}} = 0.00278 \text{ hPa}^{-1}$$

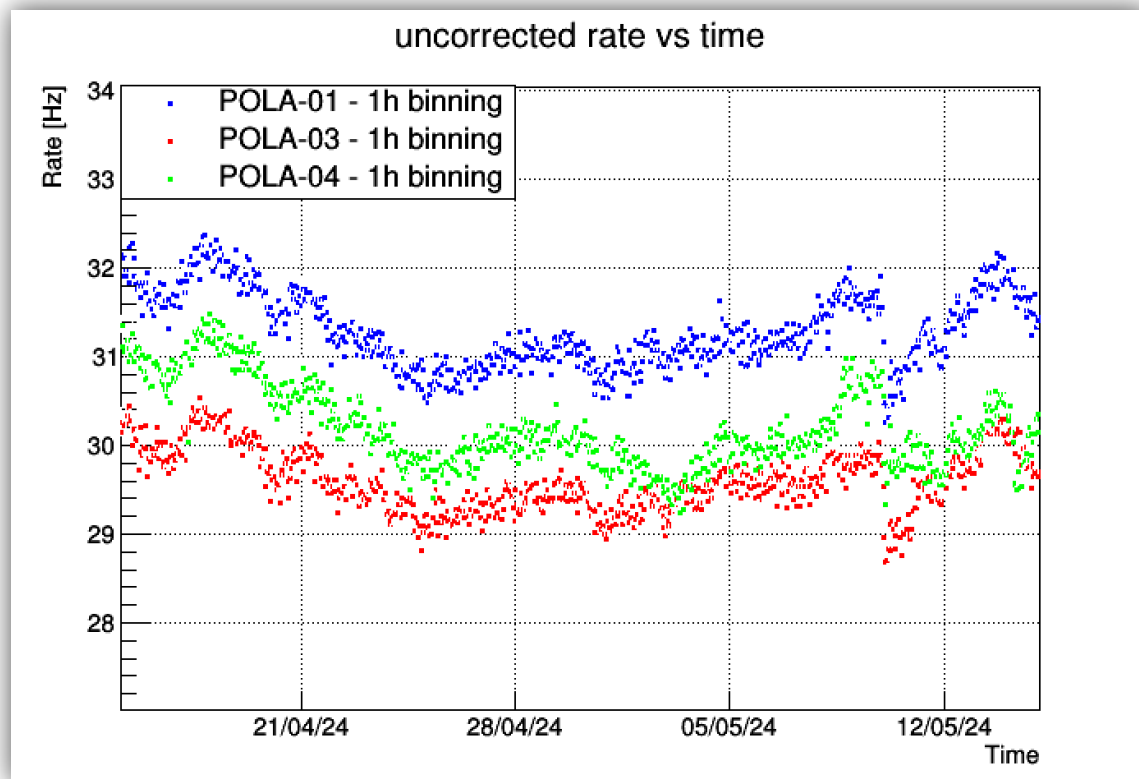
Barometric Correction



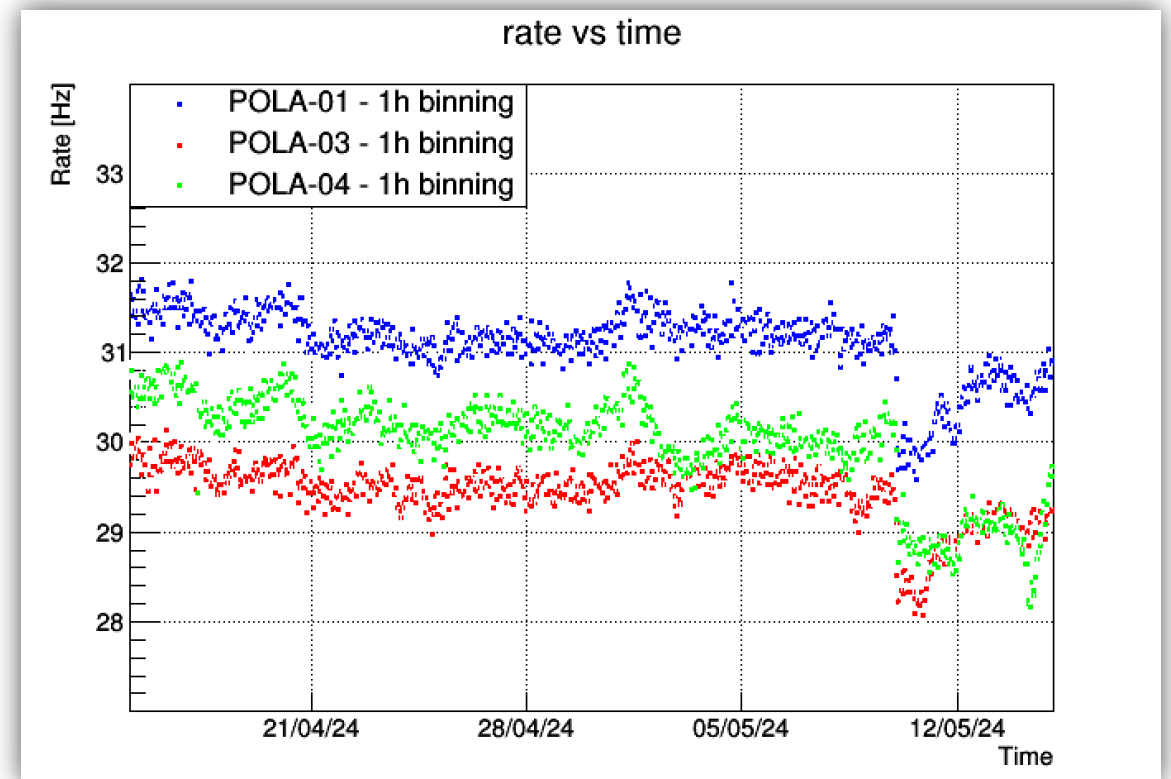
The barometric correction eliminates the linear anticorrelation between the pressure and the natural logarithm of the rate

Corrected Plots

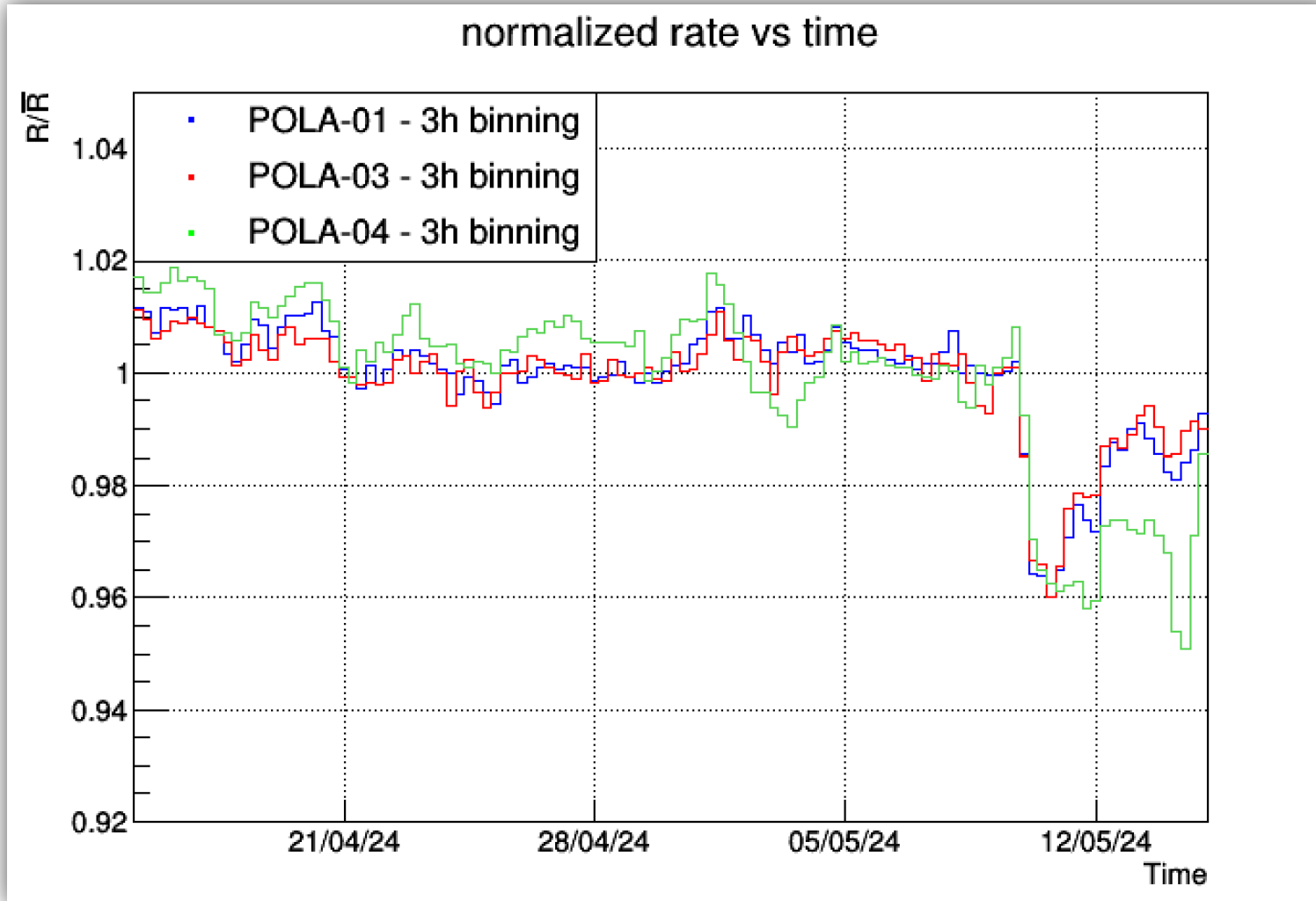
Before the correction



After the correction



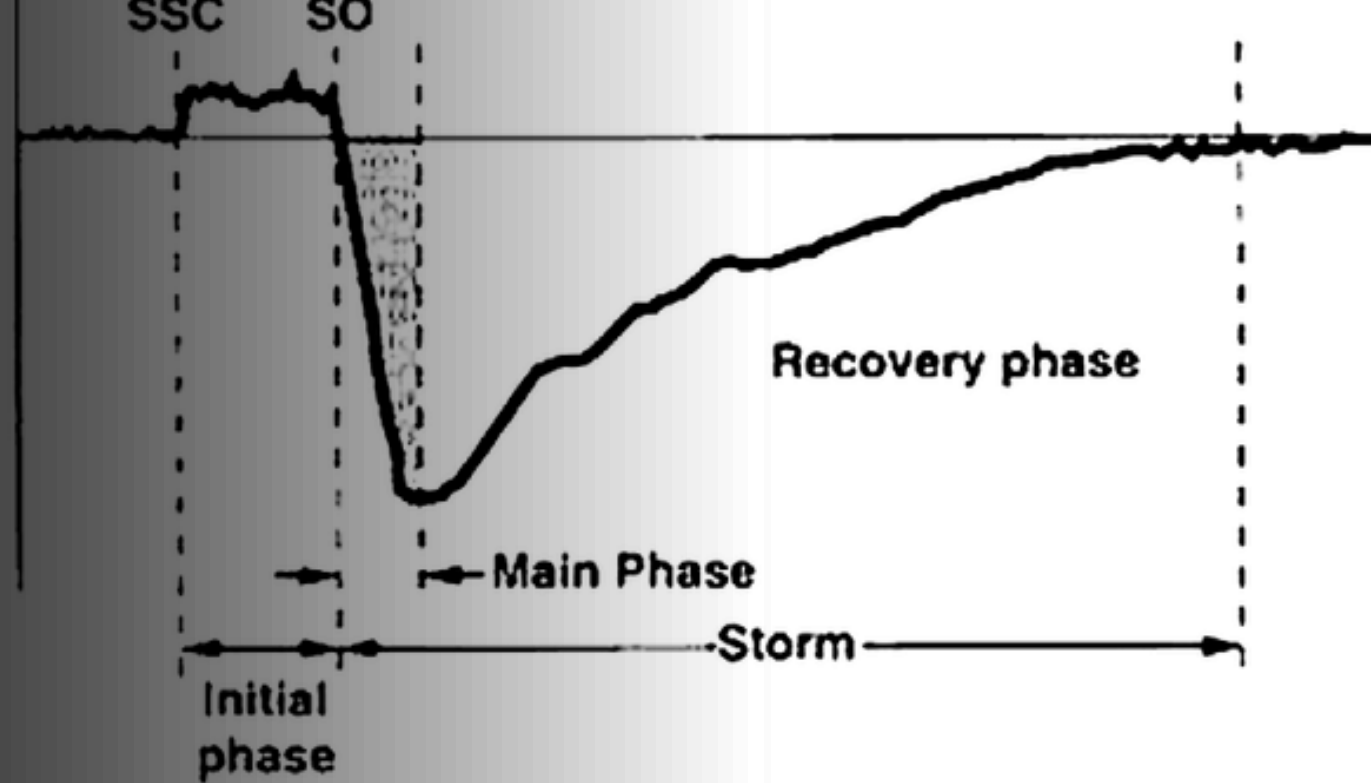
Forbush Decrease Observed by POLA 01-03-04



A Forbush decrease of approximately 4% was observed by all three telescopes and corresponds precisely to the time window of the geomagnetic storm (May 11-12, 2024).

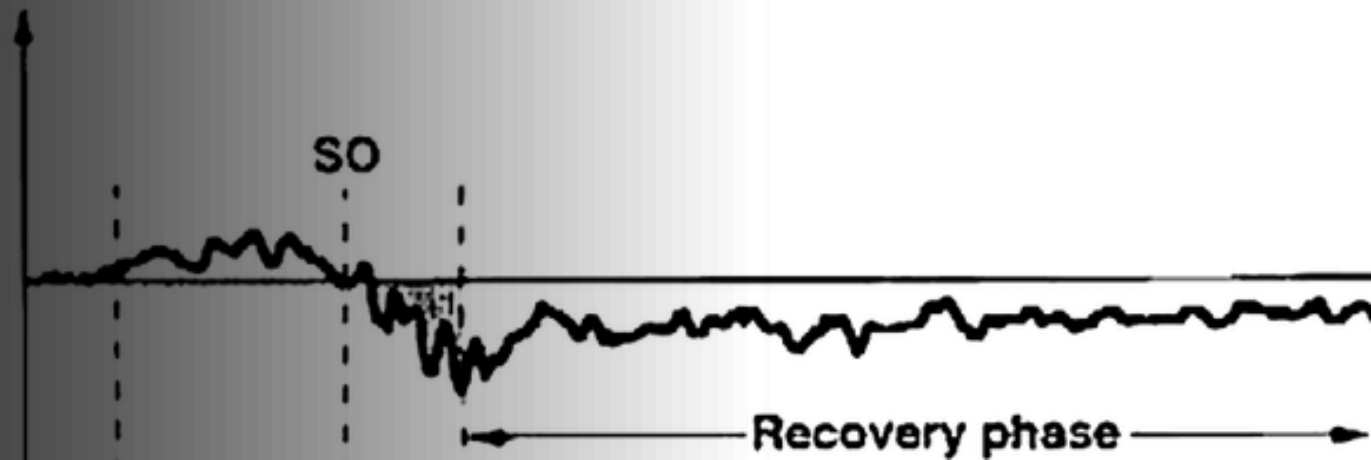
Rate vs Dst Index

Dst, nT



Solar Minimum (CIR) Storm

Dst, nT



The Dst data provided by [World Data Center for Geomagnetism, Kyoto](#)

Provisional Dst index

Note! These data are only for non-commercial purpose.

The provisional Dst index is calculated from geomagnetic field data which were visually screened for artificial noises.

Acknowledgments: We thank the geomagnetic observatories (Kakioka [JMA], Honolulu and San Juan [USGS], Hermanus [RSA], ...)

Year Month
2021 : [01](#) [02](#) [03](#) [04](#) [05](#) [06](#) [07](#) [08](#) [09](#) [10](#) [11](#) [12](#)
2022 : [01](#) [02](#) [03](#) [04](#) [05](#) [06](#) [07](#) [08](#) [09](#) [10](#) [11](#) [12](#)
2023 : [01](#) [02](#) [03](#) [04](#) [05](#) [06](#) [07](#) [08](#) [09](#) [10](#) [11](#) [12](#)
2024 : [01](#) [02](#) [03](#) [04](#) [05](#) [06](#)

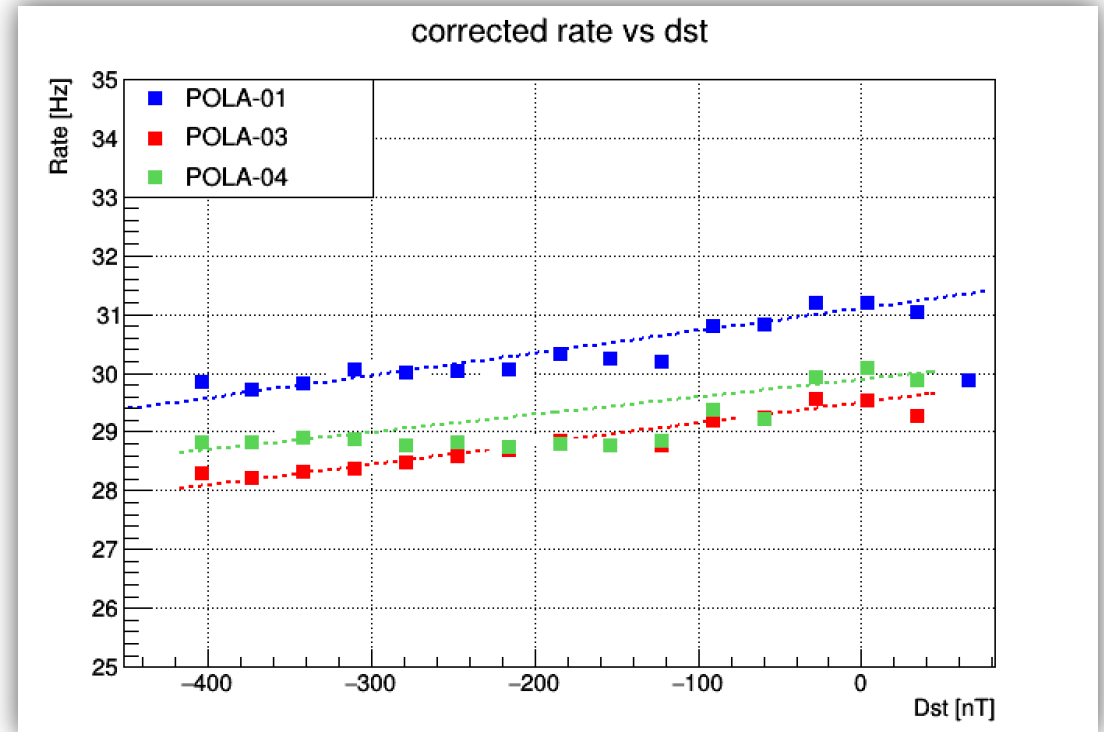
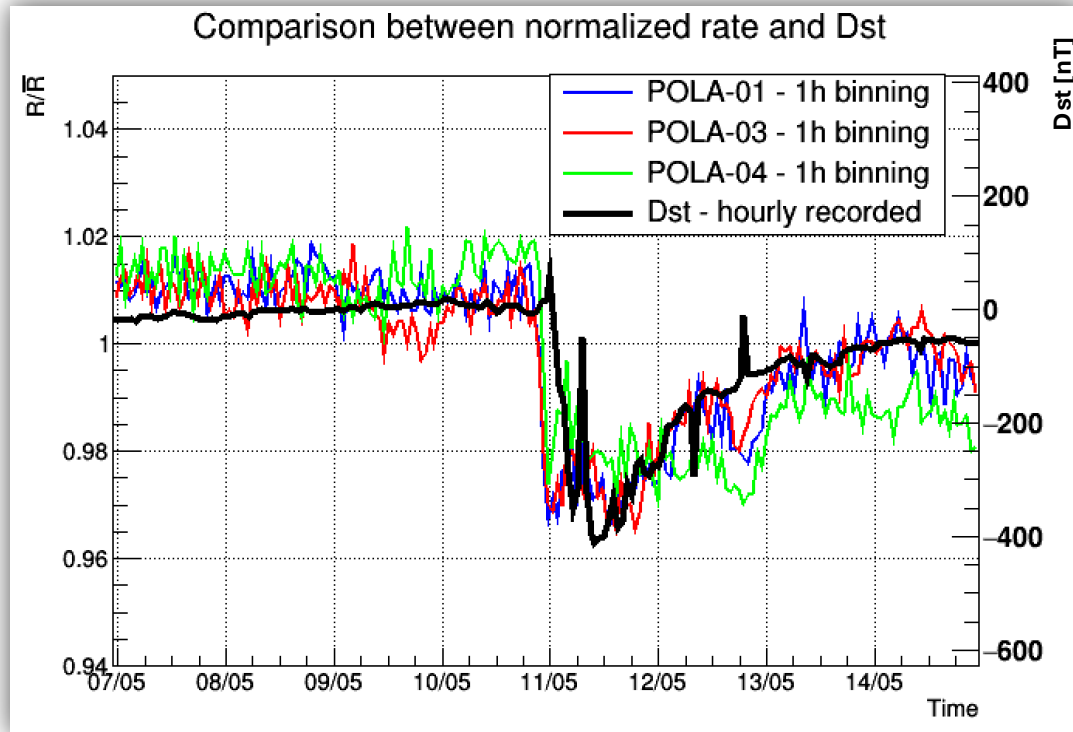
Link to [Dst index Home Page](#) | [Real-time \(Quicklook\) Dst index Page](#)

DST2405*01PPX120	0	-27	-33	-28	-15	-14	-14	-17	-14	-11	-9	-11	-11	-12	-13	-14	-9	-4	1	-2	1	5	1	1	-1	-10	
DST2405*02PPX120	0	-2	-2	5	5	3	2	-4	-4	2	7	5	-4	-9	-19	-21	-54	-78	-75	-85	-93	-96	-77	-56	-63	-30	
DST2405*03PPX120	0	-63	-60	-54	-62	-61	-60	-59	-54	-47	-44	-41	-38	-37	-37	-40	-37	-34	-33	-33	-36	-35	-32	-29	-27	-44	
DST2405*04PPX120	0	-26	-25	-23	-21	-20	-19	-19	-18	-18	-19	-18	-15	-15	-19	-22	-22	-18	-15	-12	-12	-16	-18	-14	-8	-18	
DST2405*05PPX120	0	-4	-5	-4	-8	-14	-18	-17	-9	-1	-3	0	6	12	11	11	12	11	10	11	6	-8	-28	-45	-50	-5	
DST2405*06PPX120	0	-41	-50	-42	-42	-43	-38	-29	-27	-18	-14	-10	-10	-7	-8	-13	-9	-11	-14	-15	-17	-20	-20	-20	-16	-22	
DST2405*07PPX120	0	-14	-13	-10	-14	-16	-14	-10	-4	-5	-7	-9	-10	-12	-16	-19	-18	-16	-20	-14	-12	-10	-8	-7	-7	-12	
DST2405*08PPX120	0	-5	-2	1	-3	-3	-2	-3	-1	0	0	-1	0	0	-4	-5	-5	-2	-2	1	1	-1	2	3	4	-1	
DST2405*09PPX120	0	6	10	11	8	5	3	2	3	5	6	7	11	12	13	10	8	12	16	19	18	14	10	8	6	9	
DST2405*10PPX120	0	4	3	5	13	6	-4	-3	6	5	6	5	-3	-7	-8	-1	13	18	61	-36	-135	-165	-287	-351	-318	-49	
DST2405*11PPX120	0	-322	-397	-412	-403	-399	-369	-332	-384	-373	-306	-326	-274	-265	-287	-292	-275	-277	-253	-206	-202	-197	-179	-169	-178	-295	
DST2405*12PPX120	0	-159	-149	-141	-145	-148	-154	-144	-142	-140	-123	-112	-114	-114	-112	-112	-106	-103	-98	-90	-86	-83	-86	-98	-92	-119	
DST2405*13PPX120	0	-83	-83	-89	-96	-102	-96	-96	-77	-71	-67	-65	-67	-65	-72	-68	-61	-61	-60	-58	-55	-55	-53	-55	-56	-71	
DST2405*14PPX120	0	-53	-55	-55	-58	-55	-52	-53	-53	-54	-58	-59	-59	-60	-56	-56	-54	-48	-46	-48	-48	-48	-49	-50	-51	-53	
DST2405*15PPX120	0	-50	-48	-46	-47	-42	-40	-45	-45	-42	-41	-44	-50	-52	-52	-52	-50	-46	-42	-35	-36	-43	-52	-56	-59	-46	
DST2405*16PPX120	0	-58	-58	-55	-54	-49	-40	-49	-42	-46	-82	-90	-80	-69	-81	-81	-83	-76	-72	-67	-62	-62	-62	-62	-60	-64	
DST2405*17PPX120	0	-60	-59	-57	-58	-53	-48	-51	-44	-39	-39	-37	-41	-46	-36	-34	-31	-42	-57	-69	-81	-88	-88	-96	-99	-56	
DST2405*18PPX120	0	-91	-88	-85	-85	-87	-83	-81	-76	-70	-71	-75	-74	-71	-71	-72	-72	-64	-58	-55	-53	-52	-48	-45	-45	-70	
DST2405*19PPX120	0	-43	-39	-40	-45	-48	-53	-51	-47	-44	-40	-32	-33	-31	-32	-38	-43	-41	-38	-35	-32	-23	-23	-24	-23	-37	
DST2405*20PPX120	0	-22	-22	-21	-27	-32	-30	-32	-44	-37	-32	-36	-36	-31	-26	-31	-29	-24	-22	-19	-17	-18	-19	-20	-24	-27	
DST2405*21PPX120	0	-22	-16	-17	-21	-22	-23	-22	-21	-18	-15	-17	-21	-30	-29	-26	-22	-21	-22	-17	-13	-17	-21	-25	-25	-21	
DST2405*22PPX120	0	-21	-19	-18	-19	-18	-18	-15	-14	-15	-15	-13	-11	-12	-12	-11	-7	-2	2	2	0	-2	-3	-4	-11		
DST2405*23PPX120	0	-4	-2	0	-1	0	-4	-10	-10	-16	-19	-18	-21	-20	-23	-27	-29	-32	-33	-31	-29	-28	-32	-37	-26	-19	
DST2405*24PPX120	0	-24	-22	-18	-18	-26	-36	-38	-37	-29	-30	-25	-26	-29	-32	-33	-35	-31	-31	-29	-29	-30	-28	-23	-14	-28	
DST2405*25PPX120	0	-10	-10	-13	-18	-21	-21	-20	-18	-17	-17	-16	-13	-11	-10	-12	-13	-10	-14	-17	-17	-17	-19	-27	-31	-16	
DST2405*26PPX120	0	-27	-24	-20	-19	-23	-23	-23	-21	-20	-19	-15	-15	-16	-19	-28	-28	-28	-26	-24	-31	-34	-27	-22	-17	-23	
DST2405*27PPX120	0	-14	-9	-7	-9	-10	-11	-14	-8	-9	-18	-18	-18	-10	-12	-20	-22	-18	-14	-11	-14	-14	-15	-18	-17	-14	
DST2405*28PPX120	0	-14	-13	-15	-16	-14	-9	-8	-6	0	0	0	0	-3	-8	-9	-5	2	5	8	6	0	-3	-4	-1	-4	
DST2405*29PPX120	0	1	7	8	6	6	8	4	8	13	16	16	9	9	7	6	11	20	21	16	7	5	-3	-8	-8	8	
DST2405*30PPX120	0	-7	-6	-3	-3	0	0	4	7	8	4	7	4	7	4	-3	-6	-10	-10	-10	-11	-21	-25	-27	-23	-18	-6
DST2405*31PPX120	0	-14	-11	-18	-25	-32	-32	-33	-27	-27	-30	-29	-30	-28	-29	-30	-31	-24	-25	-28	-32	-34	-34	-33	-29	-28	

[Created at Wed Oct 16 04:06:09 UTC 2024]

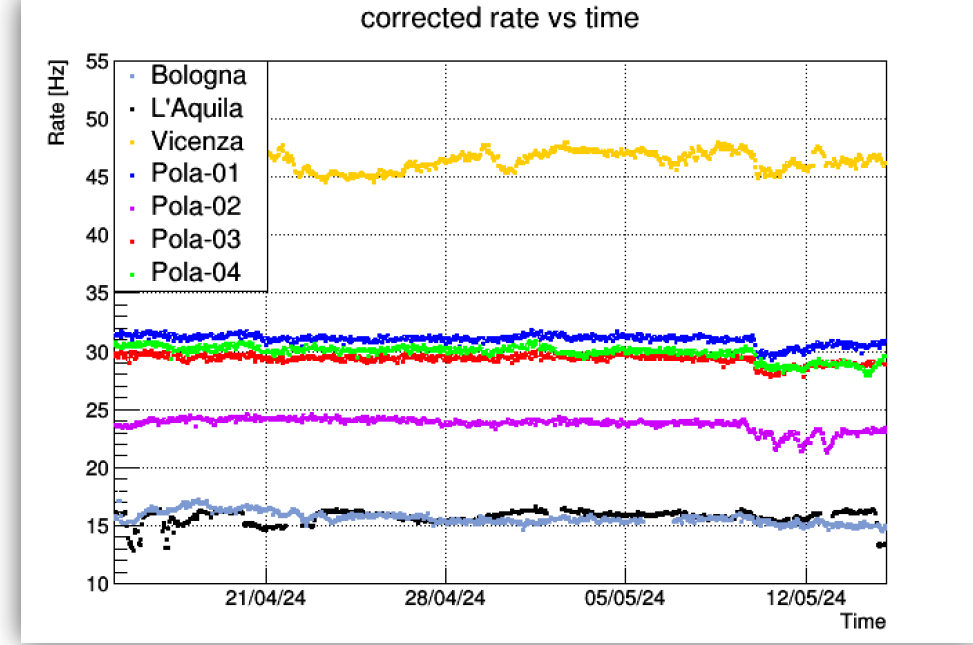
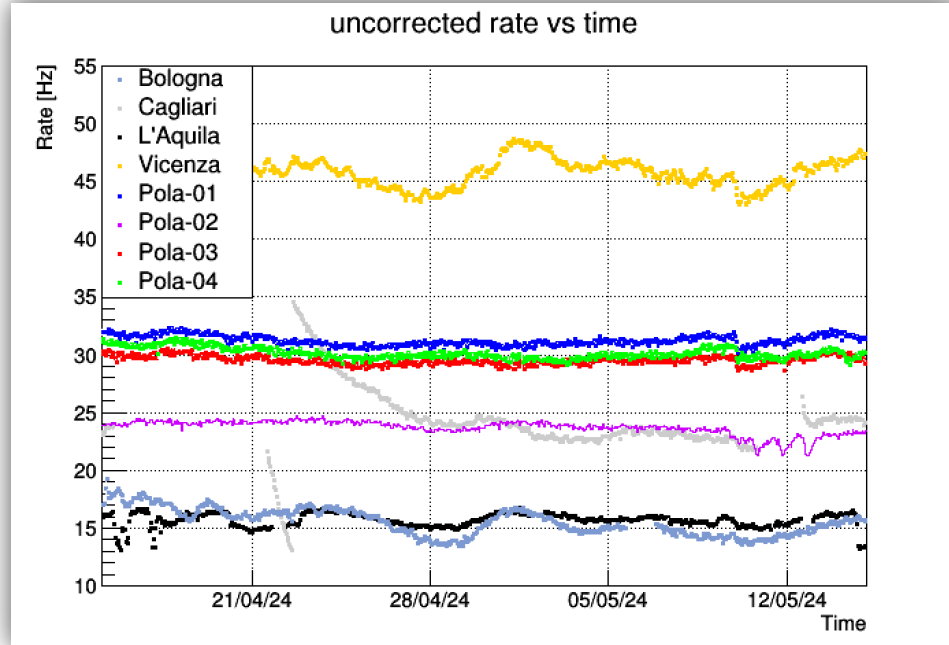
Dst values are arranged in a 31x24 matrix, where the rows correspond to the days and the columns correspond to the hours of the day

Comparison of Rate and Dst Index Trends



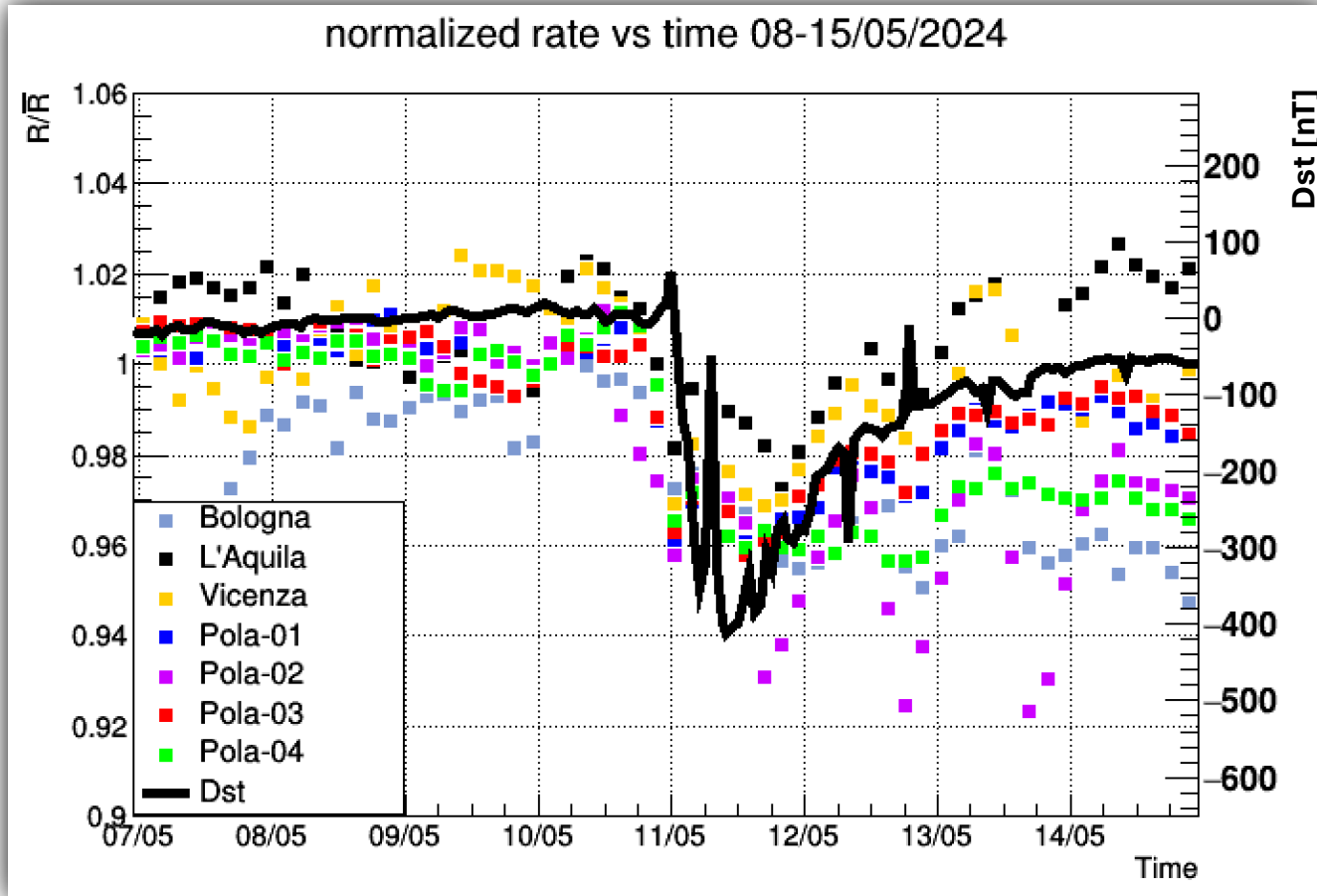
The plots of the normalized rate and dst match very well. These graphs show a strong correlation between these physical quantities, which strengthens the cause-and-effect relationship between magnetic storms and flux decrease.

Extending the Analysis with Additional EEE Telescopes



We extended the analysis to include four additional telescopes from the EEE collaboration, which, unlike Pola-01-03-04, do not clearly highlight the Forbush decrease. This is particularly true for the MRPC telescopes, currently transitioning to new gas mixtures, causing suboptimal operation, frequent interventions, and interruptions.

The FD Observed by Several Stations of the EEE Collaboration




In spite of the anomalous behavior of some telescopes, overlaying all the rate graphs allows the decrease caused by the storm to be discerned, especially if compared with the Dst trend.



Thank You

Scott E Forbush

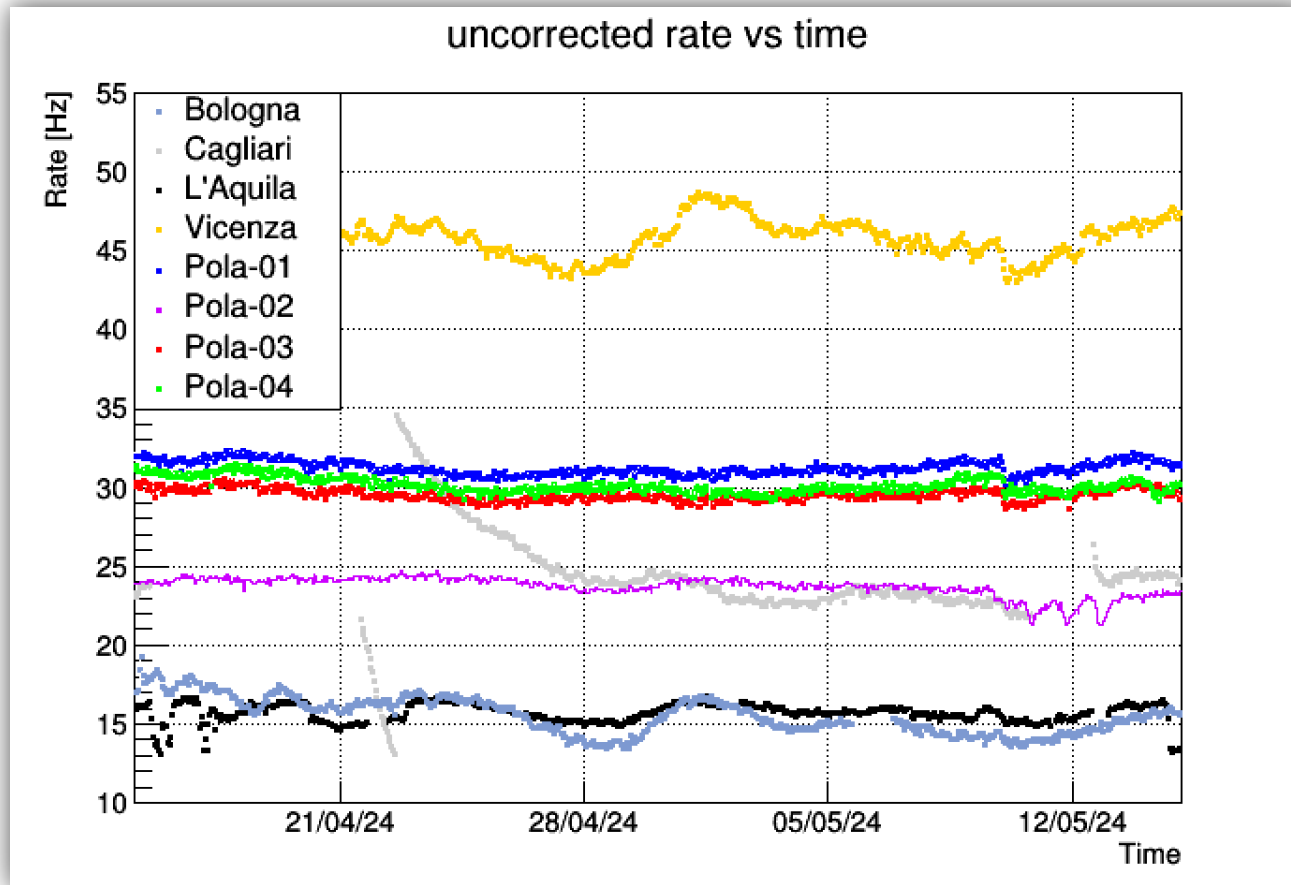


Appendix

Analysis with the whole set of telescopes

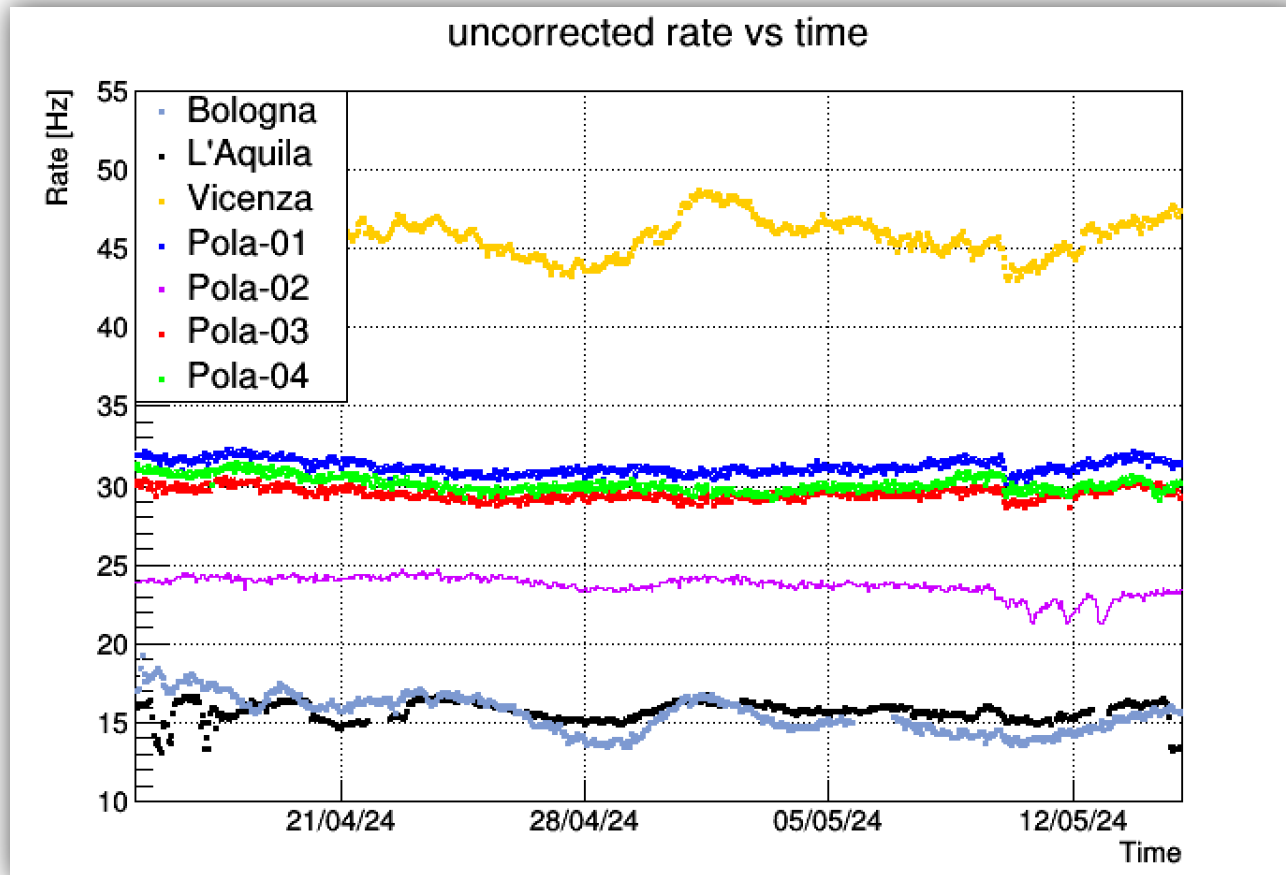


Rate of Reconstructed Tracks Plots



In some cases, the MRPC telescopes showed anomalous behavior, likely due to transitioning to new gases during the observed time window, which led to various interventions or interruptions in their operation.

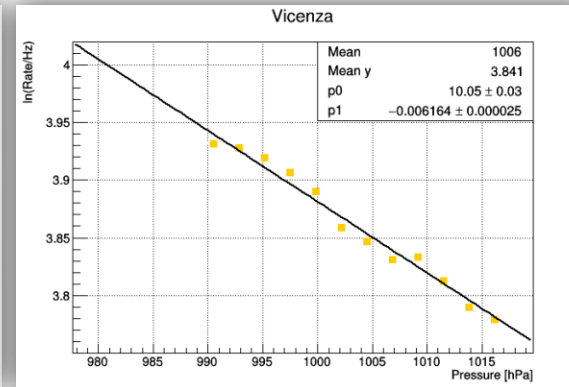
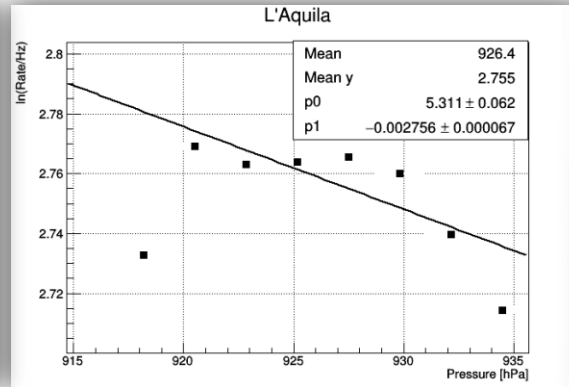
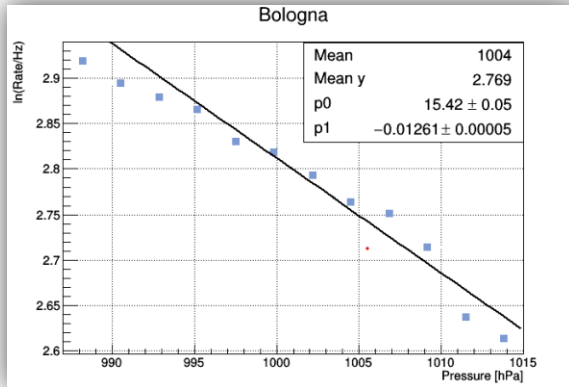
Rate of Reconstructed Tracks Plots



In some cases, the MRPC telescopes showed anomalous behavior, likely due to transitioning to new gases during the observed time window, which led to various interventions or interruptions in their operation.

The telescope that exhibited the worst behavior was the one installed in Cagliari, which is why it was excluded from our analysis.

Barometric Coefficients



$$\alpha_{\text{Bologna}} = 0.00154 \text{ hPa}^{-1}$$

$$\alpha_{\text{L'Aquila}} = 0.00304 \text{ hPa}^{-1}$$

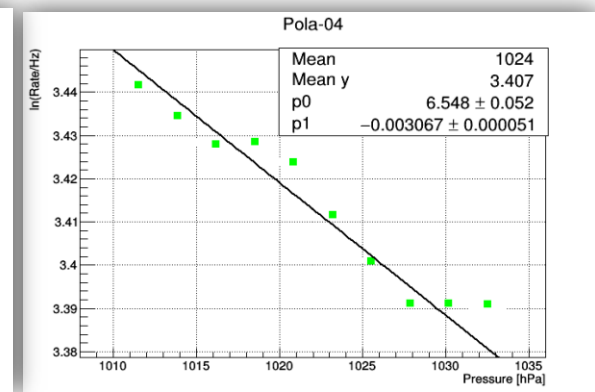
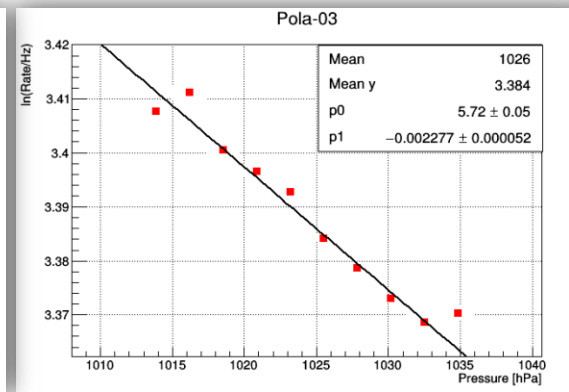
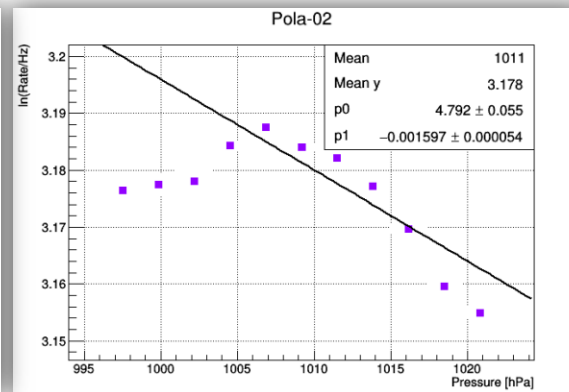
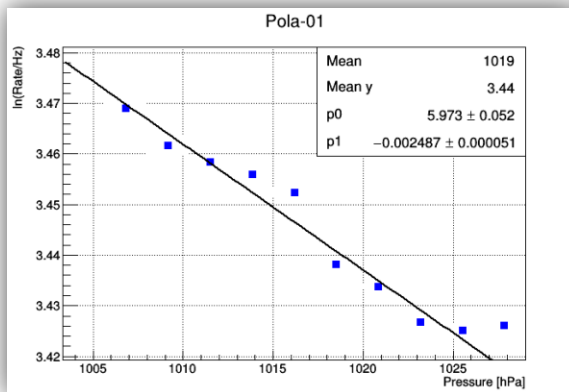
$$\alpha_{\text{Vicenza}} = 0.00634 \text{ hPa}^{-1}$$

$$\alpha_{\text{POLA01}} = 0.00250 \text{ hPa}^{-1}$$

$$\alpha_{\text{POLA02}} = 0.00157 \text{ hPa}^{-1}$$

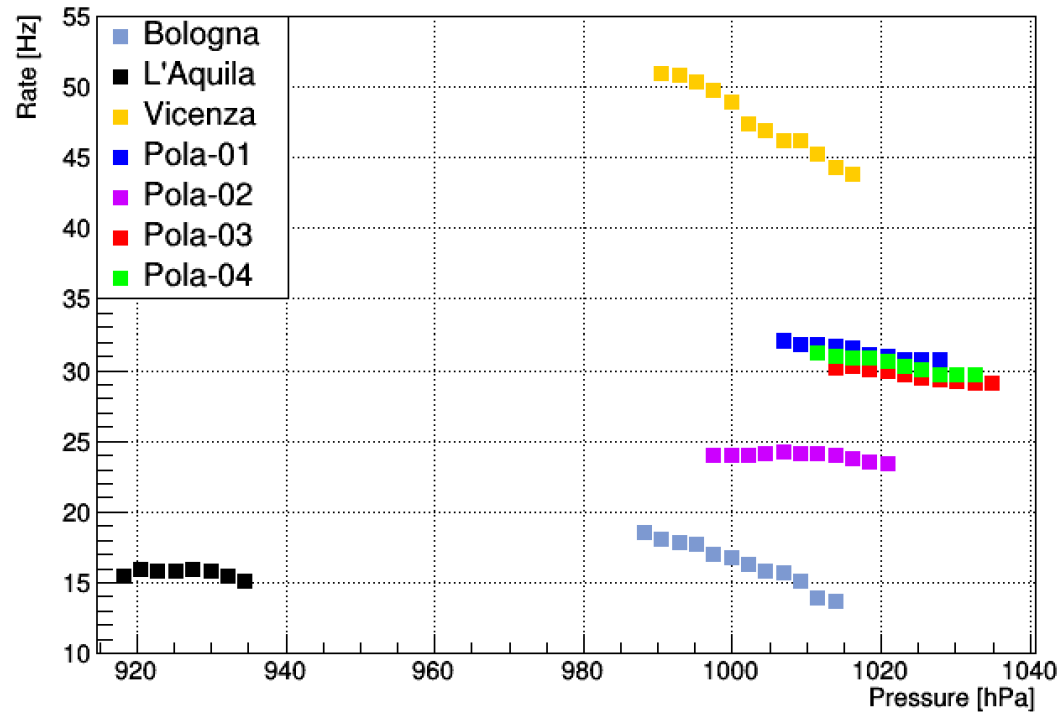
$$\alpha_{\text{POLA03}} = 0.00232 \text{ hPa}^{-1}$$

$$\alpha_{\text{POLA04}} = 0.00305 \text{ hPa}^{-1}$$

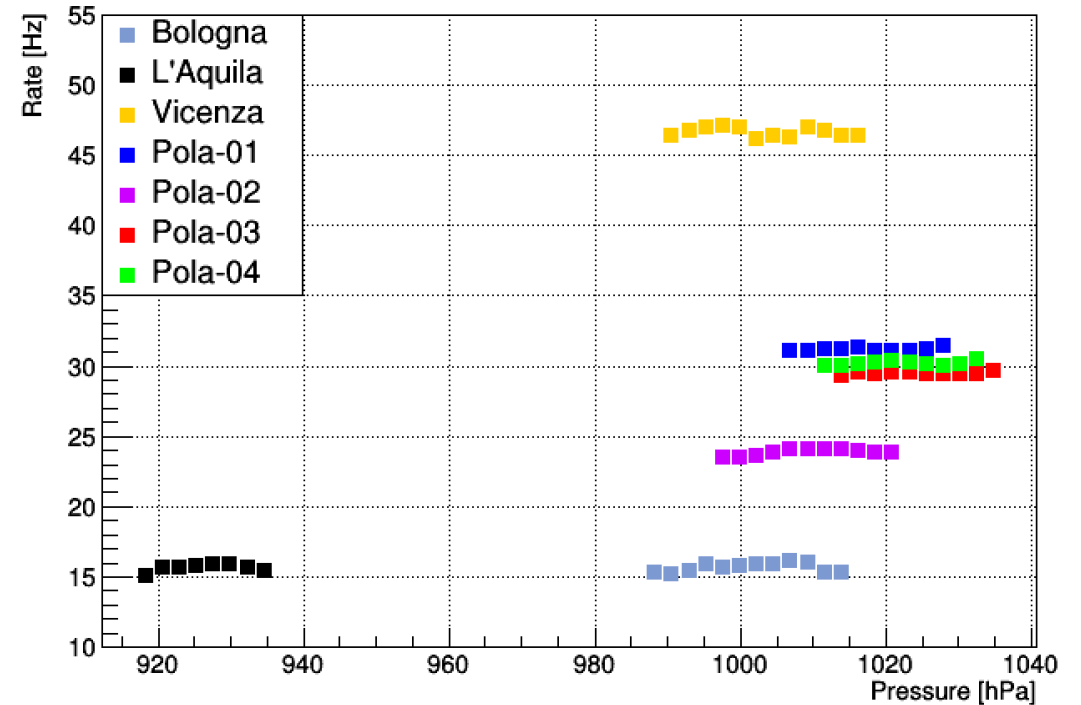


Barometric Correction

uncorrected rates vs pressure

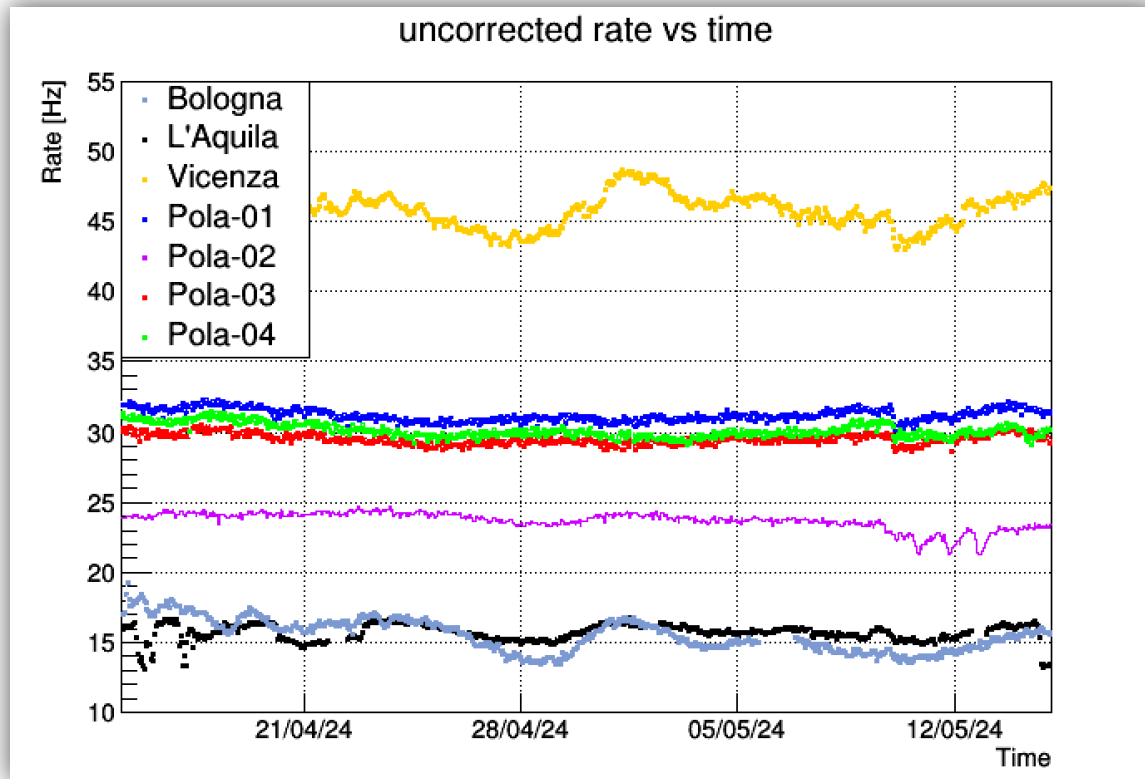


corrected rate vs pressure

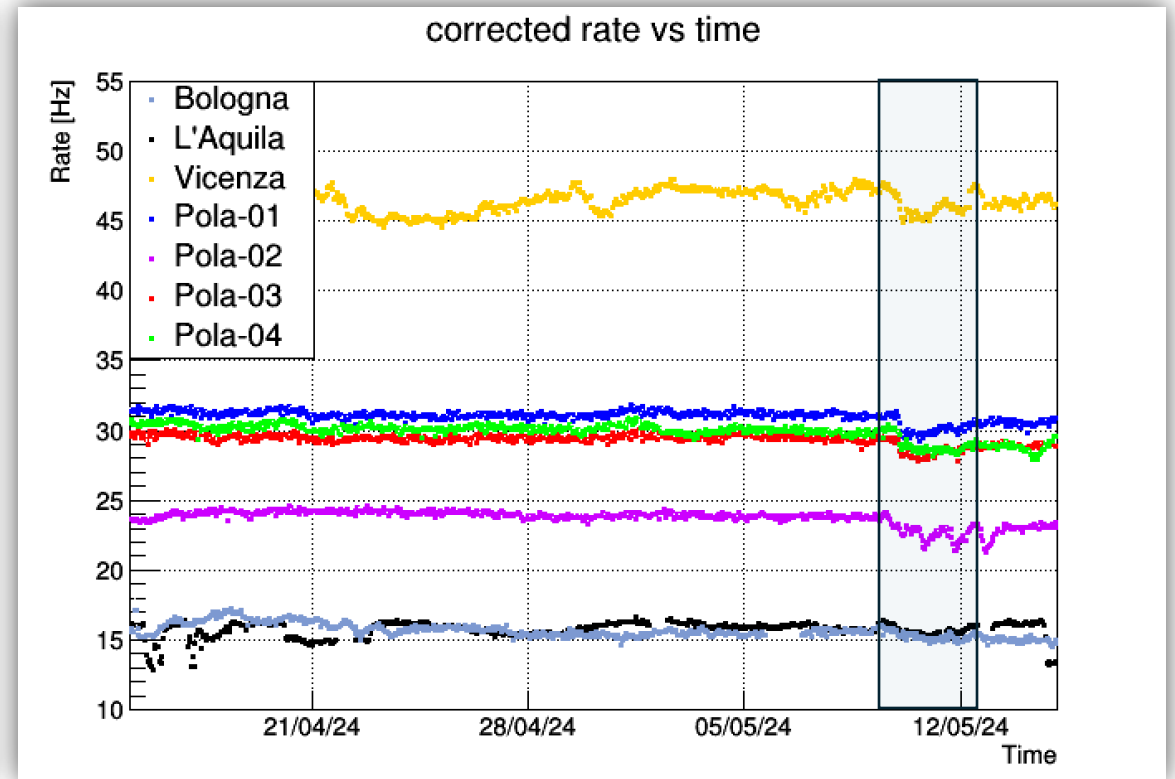


Corrected rate plots

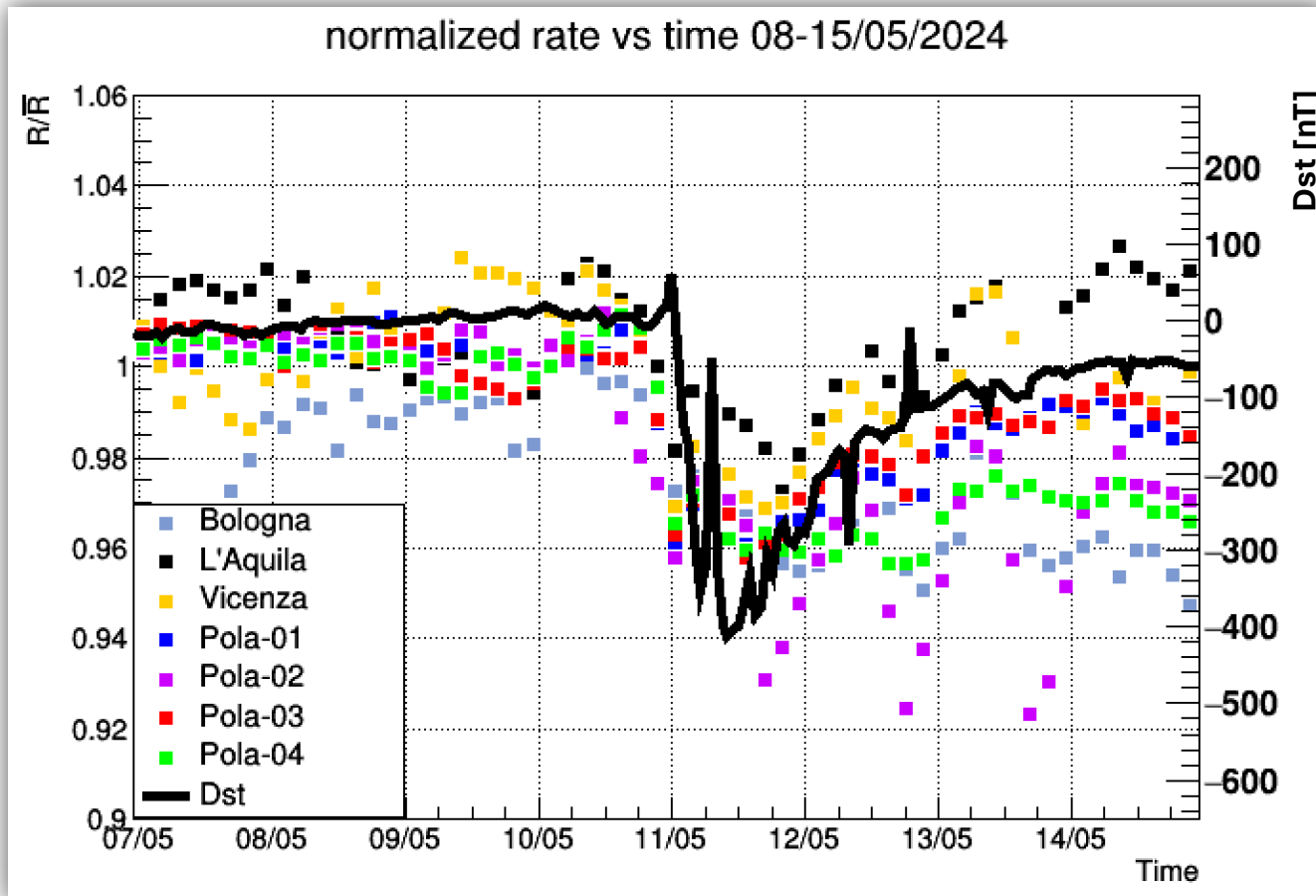
Before the correction



After the correction



The Forbush decrease observed by several telescopes of the EEE collaboration



The MRPC and Pola-02 telescopes do not highlight the Forbush decrease as clearly as the Pola-01, Pola-03, and Pola-04 detectors do. However, by overlaying all the rate graphs against time, the decrease that occurred during the storm days can be discerned.